Plasmonic Aharonov-Bohm effect: Optical spin as the magnetic flux parameter

Yuri Gorodetski, Sergey Nechayev, Vladimir Kleiner, and Erez Hasman*
Micro and Nanooptics Laboratory, Faculty of Mechanical Engineering, and Russell Berrie Nanotechnology Institute, Technion-Israel Institute of Technology, Haifa 32000, Israel
(Received 28 July 2010; published 17 September 2010)

A wave-front phase dislocation due to the scattering of surface plasmons from a topological defect is directly measured in the near field by means of interference. The dislocation strength is shown to be equal to the incident optical spin with analogy to the magnetic flux parameter in the Aharonov-Bohm effect.

DOI: 10.1103/PhysRevB.82.125433 PACS number(s): 73.20.Mf, 42.25.Ja

I. INTRODUCTION

In the celebrated paper of Aharonov and Bohm,[1] it was shown that the scattering pattern of charged particles impinging on an impenetrable cylinder depends on the magnetic flux, Φ, contained within the cylinder. In particular, the phase difference of $2\pi\alpha$ is acquired between the two parts of the particles' beam passing on different sides of the cylinder, where $\alpha=q\Phi/(2\pi\hbar)$ is the flux parameter, and q is the particles' charge. In 1980 Berry showed that although α is unobservable in quantum mechanics, this parameter reveals an interesting topology of the electrons wave function, namely, that it corresponds to the strength of wave-front dislocation (the number of wave crests ending on the dislocation).[2,3] A water wave analog of the Aharonov-Bohm (AB) experiment was presented, where the interference of a plane wave with a vortex was observed using a water ripple tank. It was shown that the water circulation corresponding to α in the AB experiment is manifested by the wave-front dislocation strength. Here, we present a direct measurement of the wave dislocation strength of the surface plasmon-polaritons (SPPs) scattered by a topological defect. A circular nanoslit was used to excite an out-propagating plasmonic wavefront. We measured the scattered plasmonic-wave dislocation strength by its interference with an additional plasmonic reference wave. The dislocation strength was shown to be equal to the incident optical spin (polarization helicity) in a manner similar to the AB wave function dislocation strength being equal to the magnetic flux parameter. Moreover, we experimentally demonstrated that the SPP wave dislocation is independent on the incident wavelength and the nanoslit diameter, therefore verifying the geometric nature of the phenomenon. This effect is attributed to the optical spin-orbit interaction (SOI)–coupling of the intrinsic angular momentum-spin and the extrinsic (orbital/linear) momentum of the electromagnetic field.[4–10] In general, SOI lies in the origin of such remarkable effects as the optical spin-Hall effect,[4,11–13] the plasmonic Coriolis effect,[14] and the optical Magnus effect.[15] Our experiment was analyzed using a rotating reference frame, which leads to a spin-dependent correction of the momentum term in the wave equation. The experiment and analysis presented in this paper elucidate the significance of the optical spin in the scattering of SPPs from a topological defect and its connection to the plasmonic phase dislocation.

II. PHASE DISLOCATIONS

Let us consider a monochromatic plane wave propagating in certain direction. The wave-fronts are defined as lines of constant phase, χ, of a complex wave, $\psi(\mathbf{r})=|\psi(\mathbf{r})|\exp[i\chi(\mathbf{r})]$. Wave crests are particular wave-fronts, defined by $\chi(\mathbf{r})=2M\pi$, where M is an integer. Under some circumstances, one may find a point such that when making a closed loop C around it, the phase changes by multiple l_d of 2π, i.e., $l_d=\frac{1}{2\pi}\oint_C\nabla\chi(\mathbf{r})\cdot d\mathbf{r}$. This point is called a phase dislocation and was first introduced in waves by Nye and Berry[2,3] using the analogy with crystal dislocations. The dislocation strength, l_d, is the number of the wave crests that end at the dislocation point. The phase in the dislocation point is indefinite, therefore, the field must vanish there. In the three dimensional wave, the dislocation points become dislocation lines and may be monitored by the zero-field amplitude.[3] The electromagnetic field phase dislocation is analogical to a vortex in fluid and the dislocation strength corresponds to the vortex circulation.[2]

III. PLASMONIC AHARONOV-BOHM EXPERIMENT

Our system consists of a thin (120 nm) gold film evaporated onto a glass substrate with a coaxial aperture milled by a focused ion beam (FEI Strata 400 s dual beam system, Ga^+, 30 keV, 48 pA; see Fig. 1). The inner and outer radii of the aperture are 365 nm and 525 nm, respectively. A 320-nm-wide slit was milled in the proximity of the coaxial aperture in order to provide a reference wave-front for the interference measurement. The element was illuminated by a tunable CW Ti:Saphire laser (Spectra-physics-3900 S) and excited surface plasmon wave was directly probed by the 150 nm aperture near-field scanning optical microscope (NSOM) tip [Multiview 2000, Nanonics Imaging; see Fig. 1(c)]. The measured fringe pattern for incident right- and left-handed circularly polarized light ($\sigma=\pm1$) at $\lambda_0=800$ nm is presented in Figs. 2(a) and 2(b). The resulting pictures appear to be asymmetric in the sense that an additional fringe emerge above or below the coaxial aperture according to the incident spin [see fringe analysis in Figs. 2(c) and 2(d)]. It can be concluded that a plasmonic wave scattered by the cylindrical defect acquires a phase-front dislocation analogous to the one obtained in a AB wave function.[1,2,16] Such a dislocation is evidence of a spiral phase front obtained by the scattered surface plasmons. In our experiment, the additional fringe appearing in the interference pattern indicates that the topological charge of the spiral phase is ±1, depending on the incident spin; therefore, the corresponding phase distribution is given by $\phi=-\sigma\varphi$, where φ, is the azimuthal angle [Fig.

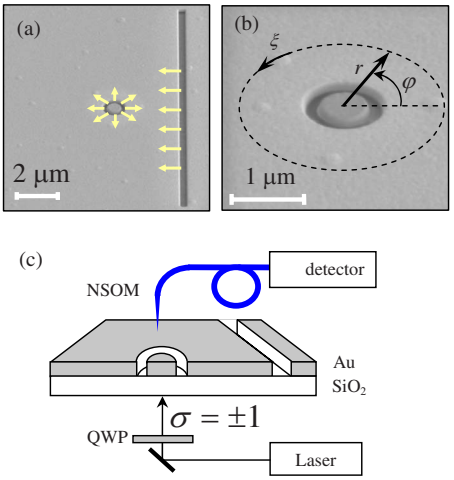

FIG. 1. (Color online) Experimental system. (a) Scanning electron microscope (SEM) picture of the investigated element (see text for details). (b) A magnified SEM picture of the circular nanoslit. (c) Experimental setup. The element was illuminated from the bottom by the laser beam whose polarization was switched by a quarter-wave plate to be $\sigma = \pm 1$. The near-field intensity distribution was measured by the NSOM tip.

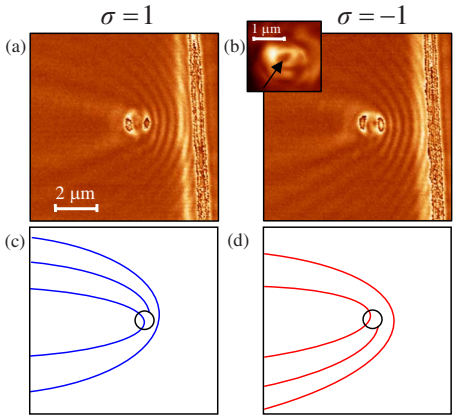

FIG. 2. (Color online) Experimentally measured near-field intensity for (a) $\sigma=1$ polarization and (b) $\sigma=-1$ polarization at $\lambda = 800$ nm. The measured fringe maxima are presented in (c) for $\sigma=1$ and (d) for $\sigma=-1$ states. The black circle in (c) and (d) represents the location of the circular nanoslit. The inset in (b) with a dark spot in the center (marked with an arrow) is the measured intensity distribution inside the circular slit.

1(b)]. This phenomenon can be elucidated by considering the effect of spin-orbit coupling.

Surface plasmon-polaritons are surface-confined electromagnetic waves due to the collective oscillations of the free electrons in metal. The coupling of light to nonradiative surface modes is achieved via momentum modification by a surface defect, such as a nanoaperture.[17,18] In particular, a one-dimensional nanoslit introduces a momentum modification (matching) in perpendicular direction, exciting a surface wave with a phase-front parallel to the slit. Moreover, only transverse magnetic polarized incident waves (with an electric field perpendicular to the slit) can be efficiently coupled by the slit to surface plasmons. This polarization selectivity in SPP excitation implies highly anisotropic interaction. Due to the circular shape of the slit in our system, it is convenient to analyze the wave propagation in a rotating reference frame attached to a local anisotropy axis.[2,19,20]

For the observer moving along a path with radius r the local structure (slit) orientation appears to be rotated with the rate $\Omega = d\theta/d\xi = 1/r$, where $\theta(\xi)$ is the slit orientation and ξ is the path parameter [see Fig. 1(b)]. The Helmholtz equation in a noninertial reference frame rotating with $\Omega(\xi)$, is $(\nabla^2 + k^2 - 2\sigma\Omega k)E_\sigma = 0$, where $E_\sigma = (E_x + i\sigma E_y)/\sqrt{2}$ are the eigenvectors of circular polarizations. Note that a spin-dependent Coriolis term appears in the corrected Helmholtz equation. This equation can be written as $(\nabla^2 + K^2)E_\sigma = 0$, where $K(\omega) \approx k(\omega) - \sigma\,\Omega$ is the *generalized momentum*.[1,2,20] A similar term also appears in the time-independent Schrödinger equation in the presence of a vector potential. This spin-dependent wave-vector modification is a manifestation of the optical spin-orbit interaction similar to the spin-Hall and the Stern-Gerlach effects. The additional momentum leads to a geometric phase accumulation of

$$\phi_g = -\int \sigma\Omega d\xi = -\sigma\theta. \tag{1}$$

Accordingly, the phase of the scattered plasmonic wave will be continuous up to the factor of 2π everywhere excluding the point $r=0$, where the phase dislocation appears. The phase in Eq. (1) is analogous to the phase arising in a AB wave function, $\psi(\mathbf{r})$.[1,2] The latter effect appears when a beam of particles with charge of q is scattered from an infinite impenetrable cylinder containing a magnetic flux $\Phi = \oint \mathbf{A}(\mathbf{r}) \cdot d\mathbf{r} = \iint \mathbf{B}(\mathbf{r}) d\mathbf{S}$, where $\mathbf{A}(\mathbf{r})$ is the vector potential and $\mathbf{B}(\mathbf{r})$ is the magnetic field. The suitable vector potential is given by $\mathbf{A}(\mathbf{r}) = (\Phi/2\pi r)\,\hat{\boldsymbol{\varphi}}$, where $\hat{\boldsymbol{\varphi}}$ is the unit vector in the azimuthal direction. The corresponding time-independent Schröedinger equation is then given by $\frac{1}{2m}[-i\hbar\nabla - q\mathbf{A}(\mathbf{r})]^2\psi(\mathbf{r}) = \frac{\hbar^2 k^2}{2m}\psi(\mathbf{r})$, where m is the particle's mass and $\hbar$ is Plank's constant. Note that the expression in parentheses is the generalized momentum term. In the linear approximation in $\mathbf{A}$, the above equation can be written as, $(\nabla^2 + k^2 - \frac{2iq}{\hbar}\mathbf{A}\cdot\nabla)\psi(\mathbf{r}) = 0$. The resulting equation resembles the Helmholtz equation in the rotating frame, where the third term in the parentheses stands for the Coriolis term. In our system, the momentum correction term along the ξ coordinate is $(\Delta k)_\xi = \sigma/r$, and is analogous to the $q\mathbf{A}$ term in the AB effect. The main result of the AB experiment is a spiral phase $\phi = \alpha\varphi$ acquired by the particles scattered from the cylinder, where the topological charge is the magnetic flux parameter. The topological charge of the phase obtained in our experiment can be found as, $l = \frac{1}{2\pi}\oint (\Delta k)_\xi d\xi = \sigma$. Therefore, one can conclude that the intrinsic spin in our experiment corresponds to the flux parameter α in the AB effect. Due to the nonzero topological charge ($\sigma = \pm 1$) a singularity of the plasmonic field appears in the center of the defect, resulting in a dark spot [see inset Fig. 2(b)]. The vanishing electromagnetic field in the center corresponds to the impenetrability of the cylinder proposed in the AB experiment.

Accordingly, the geometry of our system affects the resulting plasmonic phase-front in a similar way as a vector potential affects the electrons' wave function. In contrast to the original AB effect, here the topological charge of the plasmonic spiral phase is spin dependent, therefore it can be regarded as the intrinsic AB effect similar to the Aharonov-Casher effect.[21]

IV. GEOMETRIC NATURE OF THE EFFECT

A peculiarity of the observed effect lies in its geometric nature. The spiral phase of the plasmonic waves arises solely due to a rotation of the local anisotropy and is not the result of an optical path difference. Therefore, the phase dislocation will be independent of the wavelength or the size of the defect. To verify this, several elements with defects of different sizes were tested. In Figs. 3(a) and 3(b) we present the measured fringe patterns for circular slit with a diameter of 1.8 μm and width of 320 nm illuminated with $\lambda=800$ nm. Moreover, a simulation using a finite difference time domain (FDTD) algorithm is presented in Figs. 3(c) and 3(d) for the same defect size but for $\lambda=532$ nm incident illumination. In the measured as well as in the calculated near-field intensity distributions, same spin-dependent phase dislocations are clearly observed. A phase distribution of the scattered plasmonic field (without interfering with a reference wave) was also calculated by FDTD for $\lambda=532$ nm illumination and is presented in the Figs. 3(e) and 3(f). The topological charge of the calculated spiral phase is equal to the incident spin and is not dependent upon the incident wavelength or the defect size, emphasizing the geometric nature of the observed effect.

V. CONCLUSIONS

In summary, we have demonstrated a spin-symmetry breaking of a plasmonic field scattering from a rotationally symmetric defect by direct measurement of the near-field distribution. The spin-orbit interaction leads to a spiral spin-dependent geometric phase which was observed in our system by means of the interference with the reference plasmonic surface wave. A phase dislocation in the measured fringe pattern is analogous to the one observed in an AB effect. Moreover, both effects arise due to a scattering from a topological defect, therefore implying a strong correspondence between the equations. Our analysis sheds light on the intriguing role of optical angular momentum in scattering from topological defects which can be seen as the counterpart of the magnetic flux parameter in the AB effect.

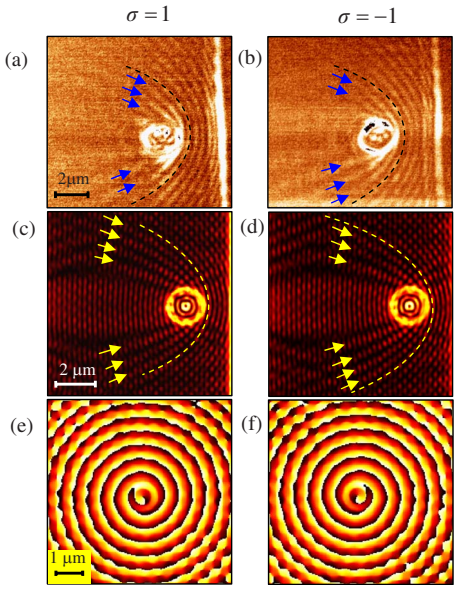

FIG. 3. (Color online) [(a) and (b)] Measured intensity distribution of the SPPs scattered from a larger diameter defect compared to Fig. 2 (see text for details) for $\sigma=1$ and $\sigma=-1$ polarizations, respectively, at $\lambda=800$ nm. [(c) and (d)] The calculated interference intensity distribution for $\sigma=1$ and $\sigma=-1$, respectively, with the same defect as in (a), now with $\lambda=532$ nm. To guide the eye, the dashed lines in (a)–(d) indicate one solid fringe and the arrows indicate the fringes appearing to the left of the dashed line. [(e) and (f)] The calculated phase distributions of the SPPs scattered from the same circular slit as in (c) and (d).

*mehasman@tx.technion.ac.il

[1] Y. Aharonov and D. Bohm, Phys. Rev. **115**, 485 (1959).
[2] M. V. Berry, R. G. Chambers, M. D. Large, C. Upstill, and J. C. Walmsley, Eur. J. Phys. **1**, 154 (1980).
[3] J. F. Nye and M. V. Berry, Proc. R. Soc. London, Ser. A **336**, 165 (1974).
[4] K. Y. Bliokh, A. Niv, V. Kleiner, and E. Hasman, Nat. Photonics **2**, 748 (2008).
[5] A. T. O'Neil, I. MacVicar, L. Allen, and M. J. Padgett, Phys. Rev. Lett. **88**, 053601 (2002).
[6] G. Biener, A. Niv, V. Kleiner, and E. Hasman, Opt. Lett. **27**, 1875 (2002).
[7] A. Niv, Y. Gorodetski, V. Kleiner, and E. Hasman, Opt. Lett. **33**, 2910 (2008).
[8] Y. Gorodetski, A. Niv, V. Kleiner, and E. Hasman, Phys. Rev. Lett. **101**, 043903 (2008).
[9] Y. Gorodetski, N. Shitrit, I. Bretner, V. Kleiner, and E. Hasman, Nano Lett. **9**, 3016 (2009).
[10] E. Brasselet, N. Murazawa, H. Misawa, and S. Juodkazis, Phys. Rev. Lett. **103**, 103903 (2009).
[11] O. Hosten and P. Kwiat, Science **319**, 787 (2008).
[12] C. Leyder, M. Romanelli, J. Ph. Karr, E. Giacobino, T. C. H. Liew, M. M. Glazov, A. V. Kavokin, G. Malpuech, and A. Bramati, Nat. Phys. **3**, 628 (2007).
[13] D. Haefner, S. Sukhov, and A. Dogariu, Phys. Rev. Lett. **102**, 123903 (2009).
[14] K. Y. Bliokh, Y. Gorodetski, V. Kleiner, and E. Hasman, Phys. Rev. Lett. **101**, 030404 (2008).
[15] A. V. Dooghin, N. D. Kundikova, V. S. Liberman, and B. Ya. Zel'dovich, Phys. Rev. A **45**, 8204 (1992).

[16] C. Coste, F. Lund, and M. Umeki, Phys. Rev. E **60**, 4908 (1999).
[17] F. López-Tejeira, S. G. Rodrigo, L. Martin-Moreno, F. J. Garcia-Vidal, E. Devaux, T. W. Ebbesen, J. R. Krenn, I. P. Radko, S. I. Bozhevolnyi, M. U. González, J. C. Weeber, and A. Dereux, Nat. Phys. **3**, 324 (2007).
[18] L. Aigouy, P. Lalanne, J. P. Hugonin, G. Julié, V. Mathet, and M. Mortier, Phys. Rev. Lett. **98**, 153902 (2007).
[19] S. G. Lipson, Opt. Lett. **15**, 154 (1990).
[20] K. Y. Bliokh, J. Opt. A: Pure Appl. Opt. **11**, 094009 (2009).
[21] Y. Aharonov and A. Casher, Phys. Rev. Lett. **53**, 319 (1984).